

Band head spin assignment of superdeformed bands in Hg isotopes through power index formula

Honey Sharma H. M. Mittal¹⁾

Dr. B.R. Ambedkar National Institute of Technology, Jalandhar, 144011, India

Abstract: The power index formula has been used to obtain the band head spin (I_0) of all the superdeformed (SD) bands in Hg isotopes. A least squares fitting approach is used. The root mean square deviations between the determined and the observed transition energies are calculated by extracting the model parameters using the power index formula. Whenever definite spins are available, the determined and the observed transition energies are in accordance with each other. The computed values of dynamic moment of inertia $J^{(2)}$ obtained by using the power index formula and its deviation with the rotational frequency is also studied. Excellent agreement is shown between the calculated and the experimental results for $J^{(2)}$ versus the rotational frequency. Hence, the power index formula works very well for all the SD bands in Hg isotopes expect for $^{195}\text{Hg}(2, 3, 4)$.

Keywords: superdeformed bands, power index formula

PACS: 21.10.Hw, 21.60.-n, 27.80.+w **DOI:** 10.1088/1674-1137/42/5/054104

1 Introduction

The presence of exotic superdeformed shapes at large deformations was predicted by Strutinsky [1]. Experimental verification of this was given in ^{152}Dy by Twin et al. [2]. The development of various detectors has helped to investigate the superdeformed (SD) bands in different mass regions, $A\sim 190, 150, 130, 80,$ and 60 . The location of SD bands in the nuclear chart can be identified by their large transition quadrupole moments and their lifetime measurements.

Various confirmations of magic number using harmonic and modified oscillator potentials were proposed by Ragnarrson et al. [3]. Subsequently, Sharma et al. [4] presented analytical data which confirm the magic numbers with various deformations, i.e. 2:1, 1:7, 1:5 for SD shapes. Experimentally, the only available data for SD bands are their intraband energies and intensities. Many attributes of SD bands, like spin predictions, parities and definite excitation energies remain undiscovered. This is due to the undiscovered linking transitions among the SD and the normal deformed (ND) bands. The spin determination has been achieved by taking theoretical models and formulae into account [5–8]. A few SD bands are also known where the spins are experimentally determined [9–16]. The SD nuclei in the $A\sim 190$ mass region show an increasing dynamic moment of inertia $J^{(2)}$ with decreasing rotational frequency [17, 18]. This is explained by the quasiparticle alignment having high N intruder

orbitals, $i_{13/2}$ proton and $j_{15/2}$ neutron, when there are pairing correlations.

Initially, SD bands in the $A\sim 190$ mass region were predicted for ^{191}Hg [19]. A SD rotational band of 12 E_γ transitions with energy spacing of 37 keV and quadrupole moment of 18 ± 3 eb was reported in ^{191}Hg . Later, superdeformation was also observed in ^{192}Hg by Becker et al. [20]. In the same year, the SD bands in ^{192}Hg were studied by Ye et al. [21], reporting 16 E_γ transitions with energy spacing of 36 keV. These SD bands also have low rotational frequency ($\hbar\omega \sim 0.125$ MeV) and spin up to 10^+ to 42^+ . A microscopic study of superdeformation in ^{193}Hg was done by Heenen et al. [22].

An investigation of the SD bands in ^{194}Hg was reported by Beausang et al. [23]. Cederwall et al. [24] also examined the features of ^{194}Hg SD bands, reporting that the $J^{(2)}$ show a decrease for $\hbar\omega \geq 0.4$ MeV and the E_γ transitions in the ^{194}Hg SD bands show evidence of staggering. The structure of SD bands in ^{195}Hg was studied by Hackman et al. [25], detecting the 4 SD bands in ^{195}Hg with a gammasphere. They also mentioned that two bands are signature partners due to the $N_{osc.} = 6$ neutron quasiparticles coupled to the SD core.

To achieve reliable spins, many theoretical models have been used, such as Harris expansion, Bohr-Mottelson expansion, the three-parameter model, the Lipas-Ejiri relation, the VMI model, the SU_q model, etc [5, 26–30]. The explanation of SD bands in odd- A and odd-odd Hg and Tl nuclei was described in the

Received 18 January 2018, Published online 11 April 2018

1) E-mail: mittal.hm@lycos.com

©2018 Chinese Physical Society and the Institute of High Energy Physics of the Chinese Academy of Sciences and the Institute of Modern Physics of the Chinese Academy of Sciences and IOP Publishing Ltd

framework of the Bohr-Mottelson two-term formula by Khalaf et al. [31]. A nuclear softness model was also introduced by Khalaf et al. [32] to study the properties of SD bands in Hg, Tl and Pb nuclei. The VMI model was used by Uma et al. [33] to predict the band head spin of SD rotational bands in the $A \sim 190$ mass region. The identification of band head spin and identical bands for odd- A nuclei in the $A \sim 190$ SD mass region was studied by Shalaby [34], using the Levenberg-Marquardt method, in which the model parameters are calculated by fitting $J^{(2)}$ with its experimental data for odd- A SD nuclei. The Harris two-parameter formula was used by Dadwal and Mittal [35] to calculate the level spin of the SD ^{195}Hg nucleus.

In this present paper we have calculated the band head spin of all the SD bands in Hg isotopes in the $A \sim 190$ mass region by using the power index formula. This study may give information about whether the power index formula is applicable in the $A \sim 190$ mass region or not. The power index formula has already proved its validity for the SD bands in $^{132}\text{Ce}(1)$ for the La and Ce isotopes [36] in the $A \sim 130$ mass region.

2 Formalism

2.1 Power index formula

To calculate the ground band level energies of a soft rotor, a formula including a single term was proposed by Gupta et al. [37]. The formula was called the power index formula. In this formula, the arithmetic mean of two terms is replaced by its geometric mean.

$$E(I) = aI^b, \quad (1)$$

where a and b are the model parameters in the power index formula and can be calculated using the least squares fitting procedure. The E_γ energies and intensities are the informational data available for the SD bands. So, we have

$$E_\gamma(I) = E(I) - E(I-2), \quad (2)$$

by using Eq. (1) and Eq. (2), we get

$$E_\gamma = a \left(I^b - (I-2)^b \right). \quad (3)$$

2.2 Dynamic moment of inertia $J^{(2)}$

Whenever the exact spins are available, the dynamic moment of inertia $J^{(2)}$ can be computed by applying the calculated transition energies [38].

$$J^{(2)} = 4000 / [E_\gamma(I+2) - E_\gamma(I)]. \quad (4)$$

3 Results and discussion

The power index formula is employed to predict the band head spins of all the SD bands in the Hg isotopes.

By using the best fit method (BFM), the parameters a and b in the power index formula are determined. The data have been taken from the tables of superdeformed nuclear bands and fission isomers given by Singh et al. [39]. The computed and the observed transition energies are in accordance with each other whenever the definite spins are available. The root mean square (rms) deviations of the computed values rely upon the proposed spins. However, if the band head spins (I_0) show a slight modification of ± 1 from the definite spin then the rms deviation increases immediately. The rms deviation may be stated as

$$\chi = \left[\frac{1}{n} \sum_{i=1}^n \left(\frac{E_\gamma^{\text{cal}}(I_i) - E_\gamma^{\text{exp}}(I_i)}{E_\gamma^{\text{exp}}(I_i)} \right)^2 \right]^{1/2}, \quad (5)$$

where n is the total number of transitions involved in the fitting procedure. The model parameters a and b of 23 SD bands in Hg isotopes evaluated from the least squares fitting technique using the power index formula are given in Table 1. The band head spins of all the SD bands in Hg isotopes are obtained by the power index formula and its comparison with other models and the experimental data are given in Table 2. The Levenberg-Marquardt method [34] and Harris two-parameter approach [35] work for the fitting of the experimental dynamic moment of inertia

Table 1. Parameters obtained from least-squares fitting of 23 bands of Hg isotopes in the $A \sim 190$ mass region using the power index formula. The numbers in parentheses are the band numbers. χ is the error in calculation.

SD band	$E_\gamma(I_0+2 \rightarrow I_0)$	a	b	$\chi \times 10^2$
^{189}Hg	366	11.1531	1.8230	0.0009
$^{190}\text{Hg}(1)$	317	11.1764	1.8124	0.478
$^{190}\text{Hg}(2)$	481	38.5929	1.5389	0.070
$^{190}\text{Hg}(3)$	318	7.9787	1.8847	0.052
$^{191}\text{Hg}(1)$	311	5.4454	1.9643	0.427
$^{191}\text{Hg}(2)$	252	8.0159	1.8813	0.504
$^{191}\text{Hg}(3)$	272	8.4912	1.8654	0.418
$^{191}\text{Hg}(4)$	281	7.0175	1.9245	0.663
$^{192}\text{Hg}(1)$	214	9.7928	1.8343	1.308
$^{192}\text{Hg}(2)$	241	9.6100	1.8256	1.386
$^{193}\text{Hg}(1)$	233	8.9943	1.8444	0.333
$^{193}\text{Hg}(2)$	254	10.356	1.8212	0.659
$^{193}\text{Hg}(3)$	234	9.0173	1.8500	0.990
$^{193}\text{Hg}(4)$	254	11.2059	1.8049	0.492
$^{193}\text{Hg}(5)$	291	6.6448	1.9225	0.784
$^{193}\text{Hg}(6)$	241	7.0031	1.9226	0.692
$^{194}\text{Hg}(1)$	212	9.9836	1.8264	1.748
$^{194}\text{Hg}(2)$	201	9.2993	1.8437	1.280
$^{194}\text{Hg}(3)$	222	9.2745	1.8443	1.036
$^{195}\text{Hg}(1)$	334	15.8235	1.7283	0.002
$^{195}\text{Hg}(2)$	274	14.8311	1.7412	0.101
$^{195}\text{Hg}(3)$	285	17.0749	1.7253	0.048
$^{195}\text{Hg}(4)$	342	7.6337	1.8880	0.008

Table 2. The band head spin (I_0) obtained from the power index formula for SD bands in Hg isotopes. The numbers in parentheses are the band numbers.

SD band	$E_\gamma(I_0+2 \rightarrow I_0)$	power index formula	Ref. [34]	Ref. [28]	Ref. [35]	Expt. [39]
^{189}Hg	366	13.5	17.5	15.5	-	14.5
$^{190}\text{Hg}(1)$	317	12	-	12	-	12
$^{190}\text{Hg}(2)$	481	12	-	23	-	12
$^{190}\text{Hg}(3)$	318	13.5	-	13	-	14
$^{191}\text{Hg}(1)$	311	15.5	15.5	13.5	-	15.5
$^{191}\text{Hg}(2)$	252	10.4	12.5	10.5	-	10.5
$^{191}\text{Hg}(3)$	272	11.3	13.5	11.5	-	11.5
$^{191}\text{Hg}(4)$	281	12	13.5	-	-	12.5
$^{192}\text{Hg}(1)$	214	8	-	8	-	8
$^{192}\text{Hg}(2)$	241	10	-	12	-	10
$^{193}\text{Hg}(1)$	233	9	-	9.5	-	9.5
$^{193}\text{Hg}(2)$	254	9.5	12.5	10.5	-	9.5
$^{193}\text{Hg}(3)$	234	9.3	11.5	9.5	-	9.5
$^{193}\text{Hg}(4)$	254	9	-	10.5	-	9.5
$^{193}\text{Hg}(5)$	291	13.3	12.5	12.5	-	13.5
$^{193}\text{Hg}(6)$	241	10	-	-	-	10.5
$^{194}\text{Hg}(1)$	212	8	-	8	-	8
$^{194}\text{Hg}(2)$	201	7.5	-	8	-	8
$^{194}\text{Hg}(3)$	222	8.5	-	11	-	9
$^{195}\text{Hg}(1)$	334	11	17.5	14.5	12.3	12.5
$^{195}\text{Hg}(2)$	274	8.5	13.5	11.5	11.4	11.5
$^{195}\text{Hg}(3)$	285	7.5	14.5	12.5	11.9	10.5
$^{195}\text{Hg}(4)$	342	12.5	17.5	15.5	15.4	15.5

Table 3. Transition energies of ^{189}Hg using the power index formula. I_0 corresponds to band head spin. $\delta = E_\gamma^{\text{exp}}(I) - E_\gamma^{\text{cal}}(I)$, where E_γ is in keV. χ is the rms deviation given by Eq. (5).

$E_\gamma^{\text{exp}}(I)$	$I_0=13$			$I_0=13.5$			$I_0=14$		
	I	$E_\gamma^{\text{cal}}(I)$	δ	I	$E_\gamma^{\text{cal}}(I)$	δ	I	$E_\gamma^{\text{cal}}(I)$	δ
366	15	366.8	-0.8	15.5	367.2	-1.2	16	367.7	-1.7
408	17	408.3	-0.3	17.5	408.4	-0.4	18	408.5	-0.5
449	19	448.9	0.1	19.5	448.4	0.6	20	448.1	0.9
489	21	488.6	0.4	21.5	488.4	0.6	22	488.1	0.9
528	23	527.5	0.5	23.5	527.2	0.8	24	527	1.0
567	25	565.8	1.2	25.5	565.5	1.5	26	565.3	1.7
604	27	603.4	0.6	27.5	603.3	0.7	28	603.2	0.8
640	29	640.4	-0.4	29.5	640.5	-0.5	30	640.6	-0.6
676	31	677.0	-1.0	31.5	677.3	-1.3	32	677.6	-1.6
χ		0.0000240286			0.00000954			0.000295654	

$J^{(2)}$. The model parameters thus obtained are used to calculate spin and also the spin may be illustrated as a function of rotational frequency $\hbar\omega$. However, the two main problems with these methods are that neither $J^{(2)}$ nor $\hbar\omega$ is calculated precisely in experiments and one has to measure their values. Secondly, these methods contain integration constants which are additional parameters. The two approaches collectively, i.e. the variation of $J^{(1)}$ and $J^{(2)}$ with angular momentum (ξ) and J_0 systematic, are used to predict the spin in Ref. [28]. The main problem with the variation of $J^{(1)}$ and $J^{(2)}$ with angular momentum (ξ), however, is that in some cases, like $^{190}\text{Hg}(4)$, $^{191}\text{Hg}(4)$, $^{193}\text{Hg}(4)$ etc, this approach does

not provide accurate spin, which may be due to the occurrence of band crossing in the plot of $J^{(2)}$ versus ξ . Similarly, for the J_0 systematic, if the spin I_0 for each band rises or falls by 1, then J_0 also rises or falls by 10%, which prevents correct prediction of the spin. In comparison to the above methods, the power index formula shows the dependence of energy on the spin, which can be determined easily from the observed rotational spectrum. Furthermore, the power index formula requires no additional parameters which cannot be measured directly from the experiment. The main advantage of the power index formula is that the only two terms of the experimental rotational spectrum can provide the values of

the two parameters which can be used to predict the energies at higher spins. One does not get a rapid change in spin by using the power index formula. Moreover, in the power index formula the variation of energy level fitting using model parameters is also less problematic.

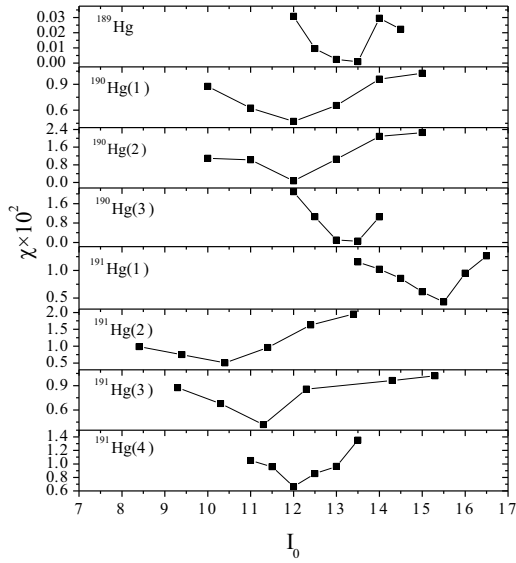


Fig. 1. χ plot to obtain band head spins of SD bands in ^{189}Hg to $^{191}\text{Hg}(4)$ isotopes using the power index formula.

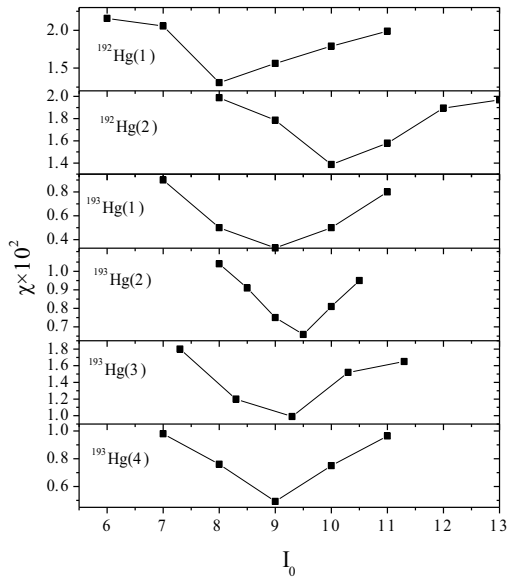


Fig. 2. χ plot to obtain band head spins of SD bands in $^{192}\text{Hg}(1)$ to $^{193}\text{Hg}(4)$ isotopes using the power index formula.

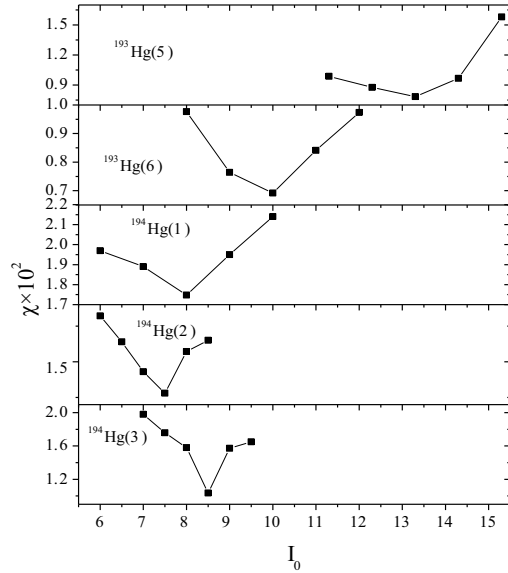


Fig. 3. χ plot to obtain band head spins of SD bands in $^{193}\text{Hg}(5)$ to $^{194}\text{Hg}(3)$ isotopes using the power index formula.

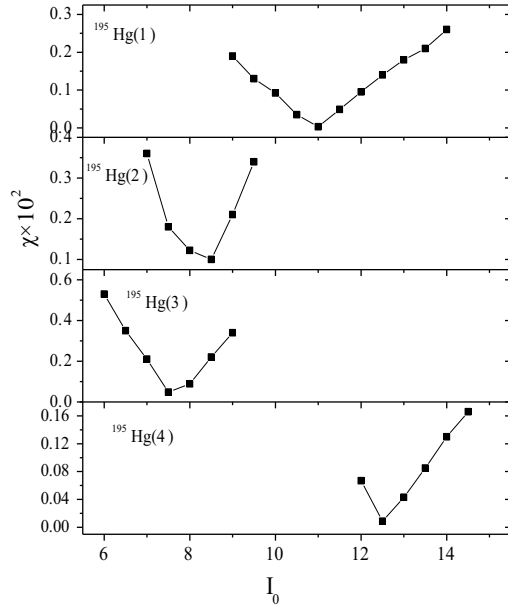


Fig. 4. χ plot to obtain band head spins of SD bands in $^{195}\text{Hg}(1)$ to $^{195}\text{Hg}(4)$ isotopes using the power index formula.

The band head spins of all the SD bands in Hg isotopes obtained by the power index formula is in accordance with the other model results and the experimental data given in the literature (see Table 2), except for $^{195}\text{Hg}(2, 3, 4)$, in which there is a difference of $3\hbar$ from the experimental data. The main possible reason may be the occurrence of significant band mixing in the energy transition levels, which could influence the root mean square deviation values while using the fitting scheme.

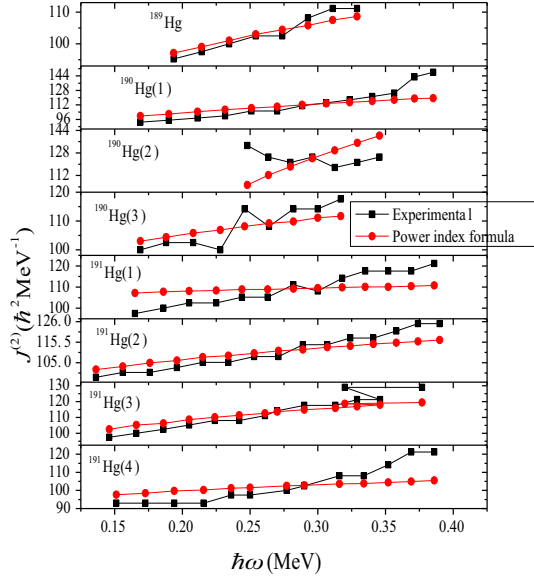


Fig. 5. (color online) Variation of calculated result of $J^{(2)}$ with $\hbar\omega$ for SD bands in ^{189}Hg to $^{191}\text{Hg}(4)$ isotopes, and comparison with experimental data.

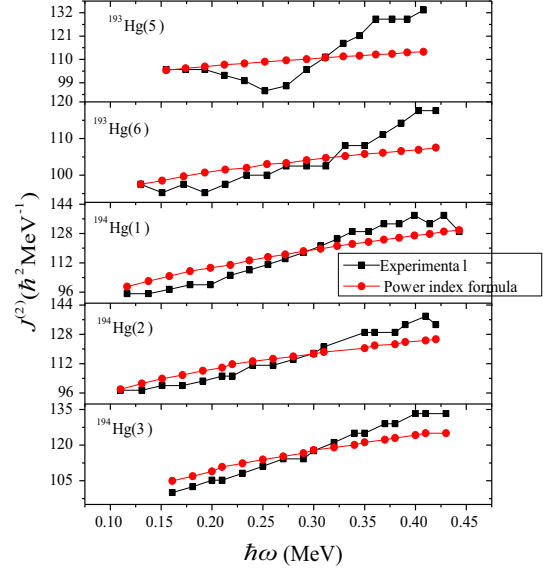


Fig. 7. (color online) Variation of calculated result of $J^{(2)}$ with $\hbar\omega$ for SD bands in $^{193}\text{Hg}(5)$ to $^{194}\text{Hg}(3)$ isotopes, and comparison with experimental data.

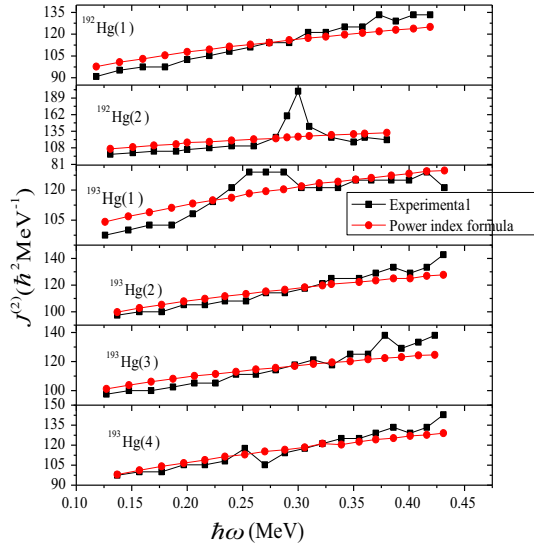


Fig. 6. (color online) Variation of calculated result of $J^{(2)}$ with $\hbar\omega$ for SD bands in $^{192}\text{Hg}(1)$ to $^{193}\text{Hg}(4)$ isotopes, and comparison with experimental data.

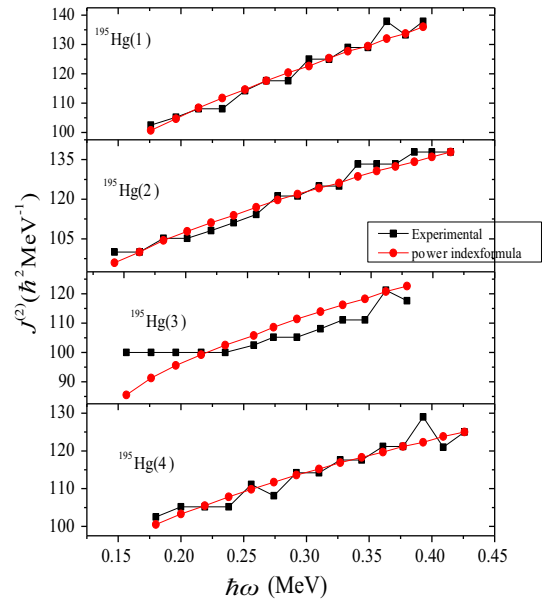


Fig. 8. (color online) Variation of calculated result of $J^{(2)}$ with $\hbar\omega$ for SD bands in $^{195}\text{Hg}(1)$ to $^{195}\text{Hg}(4)$ isotopes, and comparison with experimental data.

The band head spins of all the SD bands in Hg isotopes obtained from the χ plots using the power index formula are shown in Figs. 1–4. An explanatory example of the least squares fitting technique using the power index formula for ^{189}Hg is given in Table 3. At specified band head spins, the computed and observed transition energies are also in agreement with each other (see Table 3).

The dynamic moment of inertia $J^{(2)}$ provides guidance on the single particle configuration by taking the difference between the moments of inertia of SD bands into account. For better understanding of the single particle orbitals present in the SD bands, $J^{(2)}$ is an important measure. The inspection of the SD bands relies

on the intruder orbitals, which have a strong effect on $J^{(2)}$. As discussed in Section 1, $J^{(2)}$ displays a rapid rise with $\hbar\omega$ in the $A\sim 190$ mass region. This may be due to the arrangement of the quasiparticles of the same high N intruder i.e. $j_{15/2}$ neutrons and $i_{13/2}$ protons. The intruder orbitals involved in the different SD bands are also responsible for the structural changes. By using Eq. (4), $J^{(2)}$ can be computed. However, when we plot $J^{(2)}$ against $\hbar\omega$, a rapid rise with $\hbar\omega$ is displayed by all the SD bands in Hg isotopes (see Figs. 5–8). It is also noticed from Figs. 5–8 that the computed values of $J^{(2)}$ and the observed values of $J^{(2)}$ are in accordance with each other. Hence, from the above discussions it can be concluded that the power index formula works well in calculating the band head spin for all the SD bands in Hg isotopes in the $A\sim 190$ mass region except for $^{195}\text{Hg}(2, 3, 4)$.

4 Conclusion

In this work, we have studied the band head spin of all the SD bands in Hg isotopes by using the power index formula. The obtained results for the band head spin of all the SD bands in Hg isotopes, except for $^{195}\text{Hg}(2, 3, 4)$, are in accordance with other model results and experimental data. Whenever the exact spins are available for the SD bands, excellent agreement is obtained between the computed and the observed transition energies. A rapid rise of $J^{(2)}$ with $\hbar\omega$ is observed for the $A\sim 190$ mass region, which can be illustrated by the arrangement of the quasiparticles ($i_{13/2}$ proton and $j_{15/2}$ neutron) when there is a pairing correlation. Therefore, a similar relationship between $J^{(2)}$ and $\hbar\omega$ is obtained for all the SD bands in Hg isotopes in the $A\sim 190$ mass region. Hence, the power index formula works well in evaluating the band head spin (I_0) for all the SD bands in Hg isotopes in the $A\sim 190$ mass region except for $^{195}\text{Hg}(2, 3, 4)$.

References

- 1 V. M. Strutinsky, Nucl. Phys. A, **122**: 1-33 (1968)
- 2 P. J. Twin, B. M. Nyako, A. H. Nelson et al, Phys. Rev. Lett., **57**: 811 (1986)
- 3 I. Ragnarsson, S. G. Nilsson, and R. K. Sheline, Phys. Rev., **45**: 1 (1978)
- 4 N. Sharma, H. M. Mittal, S. Kumar et al, Phys. Rev. C, **87**: 024322 (2013)
- 5 J. A. Becker, E. A. Henry, A. Kuhnert et al, Phys. Rev. C, **46**: 889 (1992)
- 6 J. Y. Zeng, J. Meng, C. S. Wu et al, Phys. Rev. C, **44**: R1745 (1991)
- 7 R. Piepenbring and K. V. Protasov, Z. Phys. A, **345**: 7 (1993)
- 8 F. R. Xu and J. M. Hu, Phys. Rev. C, **49**: 1449 (1994)
- 9 T. L. Khoo, M. P. Carpenter, T. Lauritsen et al, Phys. Rev. Lett., **76**: 1583 (1996)
- 10 K. Hauschild, L. A. Bernstein, J. A. Becker et al, Phys. Rev. C, **55**: 2819 (1997)
- 11 A. Lopez-Martens, F. Hannachi, A. Korichi et al, Phys. Lett. B, **380**: 18 (1996)
- 12 M. J. Brinkman, J. A. Becker, I. Y. Lee et al, Phys. Rev. C, **53**: R1461 (1996)
- 13 G. Hackman, T. L. Khoo, M. P. Carpenter et al, Phys. Rev. Lett., **79** : 4100 (1997)
- 14 A. Atac, M. Piiparinen, B. Herskind et al, Phys. Rev. Lett., **70**: 1069 (1993)
- 15 C. H. Yu, C. Baktash, J. Dobaczewski et al, Phys. Rev. C, **60**: 031305(R) (1999)
- 16 C. E. Svensson, D. Rudolph, C. Baktash et al, Phys. Rev. Lett., **82**: 3400 (1999)
- 17 M. A. Riley, D. M. Cullen, A. Alderson et al, Nucl. Phys. A, **512**: 178-188 (1990)
- 18 M. W. Drigert, M. P. Carpenter, R. V. F. Janssens et al, Nucl. Phys. A, **530**: 452-474 (1991)
- 19 E. F. Moore, R. V. F. Janssens, R. R. Chasman et al, Phys. Rev. Lett., **63**: 360 (1989)
- 20 J. A. Becker, N. Roy, E. A. Henry et al, Phys. Rev. C, **41**: R9(R) (1990)
- 21 D. Ye, R. V. F. Janssens, M. P. Carpenter et al, Phys. Rev. C, **41**: R13(R) (1990)
- 22 P. H. Heenen, P. Bonche, H. Flocard et al, Nucl. Phys. A, **588**: 490-500 (1995)
- 23 C. W. Beausang, E. A. Henry, J. A. Becker et al, Z. Phys. A, **335**: 325-330 (1990)
- 24 B. Cederwall, R. V. F. Janssens, M. J. Brinkman et al, Phys. Rev. Lett., **72**: 3150 (1994)
- 25 G. Hackman, R. Krucken, R. V. F. Janssens et al, Phys. Rev. C, **55**: 148 (1997)
- 26 J. Meng, C. S. Wu and J. Y. Zeng, Phys. Rev. C, **44**: 2545 (1991)
- 27 C. S. Wu, J. Y. Zeng, Z. Xing et al, Phys. Rev. C, **45**: 261 (1992)
- 28 S. X. Liu and J. Y. Zeng, Phys. Rev. C, **58**: 3266 (1998)
- 29 D. Bonastros, S. B. Drenska, P. P. Raychev et al, J. Phys. G: Nucl. Part. Phys., **17**: L67 (1991)
- 30 Y. Liu, J. Song, H. Z. Sun et al, J. Phys. G: Nucl. Part. Phys., **24** : 117-124 (1998)
- 31 A. M. Khalaf, K. E. Abdelmageed, and E. Saber, International Journal of Theoretical and Applied Sciences, **6**: 47-56 (2014)
- 32 A. M. Khalaf, N. Mansour, M. M. Taha et al, Journal of Applied Phys., **7**: 1-11 (2015)
- 33 V. S. Uma, A. Goel, A. Yadav et al, Pramana Journal of Phys., **86**: 185-190 (2016)
- 34 A. S. Shalaby, Commun. Theor. Phys., (Beijing, China) **41**: 454 (2004)
- 35 H. M. Mittal and A. Dadwal, Proceedings of the DAE-BRNS Symp. on Nucl. Phys., **60**: 132-133 (2015)
- 36 H. Sharma and H. M. Mittal, Chinese Physics C, **41**: 124105 (2017)
- 37 J. B. Gupta, A. K. Kavathekar, and R. Sharma, Phys. Scr., **51**: 316 (1995)
- 38 X. L. Han and C. L. Wu, At. Data Nucl. Data Tables, **73**: 43 (1999)
- 39 B. Singh, R. Zywna, and R. B. Firestone, Nuclear Data Sheets, **97**: 241-592 (2002)